

SEISMIC RISK AS EXPRESSED BY ACCELERATION RESPONSE
OF SINGLE-DEGREE-OF-FREEDOM SYSTEM

By

Tsuneo KATAYAMA^{I)}

SYNOPSIS

The feasibility of seismic risk analysis in terms of acceleration response spectra was examined by several illustrative example calculations. The result of the statistical analysis of 277 acceleration response spectra conducted by the author, Iwasaki and Saeki (Bull. ERS, No.11) was used as the attenuation law. The seismic risk thus evaluated was found to more clearly show the seismic environment of a site with respect to earthquake engineering purposes than the ordinary seismic risk in terms of some peak amplitude of ground motion. The preliminary analysis has indicated that the seismic risk of long-period structures is more uniformly distributed over the whole area of Japan than that of short-period structures.

METHOD OF ANALYSIS, SEISMICITY DATA AND ATTENUATION LAW

The method of analysis and the seismicity data used for this study are described in Ref.(1). The attenuation law which describes the acceleration response spectrum in terms of earthquake magnitude, epicentral distance and site conditions are reported in detail in Refs.(2) and (3).

The area surrounding a site is divided into five distance categories $D_1 \sim D_5$ as shown in Table 1. The earthquakes occurring in each of the five distance categories are classified into five magnitude categories also shown in Table 1. The upper bound of distance category D_5 was altered to 350 km from the previous value of 400 km which was used in Ref.(1). This value of upper bound was considered more appropriate by taking account of the properties of the original data set used for the statistical analysis described in Refs.(1) and (2).

The 25 earthquake sources thus formed by the combinations of the distance and magnitude categories were assumed to be independent. The earthquake occurrence in each source ij (distance category D_i and magnitude category M_j) was assumed Poisson-distributed with a mean occurrence rate ν_{ij} , which was determined from

I) Institute of Industrial Science, University of Tokyo.

the seismicity data of Japan as described in Ref.(1).

The result of the statistical analysis(2,3) of 277 acceleration response spectra was used as the attenuation law in the present study. Modification to the raw outputs from the statistical analysis was kept minimal. The weighting factors(2,3) for the distance category D4 ($120 \text{ km} \leq \Delta < 200 \text{ km}$) at periods $T = 0.1, 2.0, 2.5, 3.0$ and 4.0s were raised to 1.00, which was considered more plausible than the original values from the statistical analysis. The uncertainty of the attenuation law was incorporated through the empirical distribution of the ratio between the observed and the predicted spectral amplitude, which was found to be log-normally distributed. This distribution is given by the following equation regardless of the natural period T of the SDOF system:

$$f(\alpha) = \frac{1}{\sqrt{2\pi}\zeta\alpha} \exp\left[-\frac{1}{2}\left(\frac{\ln\alpha - \lambda}{\zeta}\right)^2\right] \quad (1)$$

where

$$\alpha = \frac{\text{Observed spectral amplitude}}{\text{Predicted spectral amplitude}}$$

$$\lambda = E(\ln \alpha) = \ln m_\alpha - \frac{1}{2}\zeta^2$$

$$\zeta = \sqrt{\text{Var}(\ln \alpha)} = \sqrt{\ln\left[1 + \left(\frac{\sigma_\alpha}{m_\alpha}\right)^2\right]}$$

$$m_\alpha = \text{Mean of } \alpha = 1.267$$

$$\sigma_\alpha = \text{Standard deviation of } \alpha = 1.025$$

By using the attenuation law and the distribution of α described above, the probability $q_{ij}(y)$ that the acceleration response spectral amplitude SA of a structure with period T and damping factor $h = 0.05$ on a certain ground condition (GC) at the site under consideration exceeds y by the occurrence of an earthquake in source ij may be evaluated:

$$q_{ij}(y) = P(\text{SA} > y \mid T, \text{GC}, E_{ij}) \quad (2)$$

where E_{ij} denotes the event that an earthquake occurs in source ij . Then, the probability of SA exceeding y in t years may be expressed by the following equation:

$$P(SA > y \mid t) = 1 - \exp[-t v(y)] \quad (3)$$

where

$$v(y) = \sum_{i=1}^5 \sum_{j=1}^5 v_{ij} q_{ij}(y) \quad (4)$$

A number of different response spectra may be derived from Eq. (3) and the relative contributions from different earthquake sources may be evaluated by examining each of the 25 terms on the right-hand side of Eq. (4).

Generally speaking, an acceleration response spectral amplitude SA in this study carries five parameters as follows:

$$SA = SA(T, h, GC, t, p) \quad (5)$$

where

T = Natural period of SDOF system (s)

h = 0.05 = Damping factor of SDOF system

GC = Ground condition of the site

t = Length of time to be analyzed (years)

p = Probability of being exceeded

Note that the damping factor of a SDOF system is fixed at 0.05. Although the results shown in this paper were obtained by assuming the site ground condition of Type II (diluvium),^(2,3) they may be easily scaled to obtain spectra for other ground conditions. The scaling factors calculated from the results of the statistical analysis^(2,3) are shown in Fig. 1.

APPLICATION (I)

The expected acceleration response spectra ($p=0.632$) for $t=75$ years were obtained for five sites in Japan. They are

Sapporo 43°00'N, 141°20'E

Sendai 38°10'N, 140°50'E

Tokyo 35°30'N, 139°50'E

Kyoto-Osaka 34°50'N, 135°40'E

Kita-Kyushu 33°50'N, 130°40'E

Fig. 2 shows the spectra for these five sites. Although the general shapes of the spectra are similar, close examination of Fig. 2 reveals the differences in the seismic risks at these sites. The expected spectral amplitude for Tokyo is significantly greater than that for Sendai in the short-period range. For example, the expected spectral amplitude at Tokyo for structures with $T=0.2s$ is about 900 cm/s^2 , and that for Sendai is about 700 cm/s^2 . However, this difference almost diminishes in the long-period range. Similar trend may be found between the expected spectra of Kyoto-Osaka and Sapporo. On the contrary, the expected spectra for Sapporo and Kita-Kyushu are close each other for period less than $0.3s$, but those at period longer than $1.0s$ show consistent difference. These characteristics of expected spectra are attributed to the differences in the natures of seismicity of the areas surrounding the five sites investigated. Since the spectral nature of strong ground motion is affected by the magnitude and distance of a causative earthquake, the seismicity including the numbers, sizes and locations of earthquakes is reflected in the expected spectrum.

As mentioned previously, each term on the right-hand side of Eq.(4) represents the relative contribution to the total seismic risk from respective earthquake source. Table 2 summarizes the relative contributions (in percent) of earthquakes in different distance categories. For example, the seismic risk of short-period structures in Tokyo is dominantly governed by the earthquakes in categories D1 and D2, namely those with epicentral distances less than 60 km , whereas the contribution from longer-distance earthquakes (D4 and D5) becomes increasingly more important for the seismic risk of long-period structures. It is also interesting to compare the case of Tokyo with that of Sapporo. The seismic risk at Sapporo is in general more influenced by the earthquake occurring at distances farther than 120 km (categories D4 and D5). This is, however, most pronouncedly observed for the structures with natural periods longer than say $1.0s$, for which $2/3$ or more of the total risk is attributed to the earthquakes in categories D4 and D5. It is possible from Table 2 to compare, from the earthquake engineering point of view, the differences in the seismic environments of the five sites investigated, which are clearly reflected in the acceleration response spectra shown in Fig. 2.

APPLICATION (II)

As a preliminary study for the seismic risk analysis of the whole Japan area, twenty sites as shown in Fig. 3 were chosen and

their seismic risks were analyzed in detail in terms of acceleration response spectra.

As seen in Eq.(5), many acceleration spectra may be constructed for various combinations of t and p . Fig. 4 and 5 illustrate some examples of the response spectra computed for Tokyo for several combinations of t and p . Fig. 6 shows the variation of the acceleration response spectral amplitude of a $T=0.2s$ SDOF system ($h=0.05$) on $GC=II$ (diluvium) ground in Tokyo.

Although the spectral amplitude is a complicated function of t and p , it was found from the present analysis of the 20 sites that the following approximations may be used for engineering purposes:

$$SA(t,p) = 0.25 t^{0.32} SA(t=75,p) \quad (6)$$

$$\text{for } 25 \leq t \leq 200$$

$$SA(t,p) = (2.2-3.1p+1.9p^2) SA(t, p=0.632) \quad (7)$$

$$\text{for } 0.1 \leq p \leq 0.7$$

These formulas may be used for an arbitrary value of T . Therefore, when $SA(t=75, p=0.632)$ which is the expected acceleration response spectrum for the return period of 75 years is known, the spectrum for an arbitrary combination of t and p may be easily scaled by using Eqs.(6) and (7).

Table 3 summarizes the expected response accelerations for $T=0.2, 1.0$ and $4.0s$ at the 20 sites investigated. It is especially interesting to compare the two sets of values listed in columns (5) and (9). These columns show the ratios of the expected response acceleration at a site to that of Tokyo for structures with period $T=0.2$ and $4.0s$, respectively. The values in column (9) are noted to be greater than the corresponding values in column (5) except for one case. This seems to indicate that the seismic risk of long-period structures shows less local variation than that of short-period structures. This may be accounted for by the fact that the risk of long-period structures are more strongly governed by the occurrences of large, long-distance earthquakes. It is also noted that the difference between the values in columns (5) and (9) is generally greater for sites in the northern part of Japan where the large earthquakes occurring off the Pacific coast along the island arc dominate the seismic environment.

CONCLUDING REMARKS

A method of evaluating the seismic risk in terms of acceleration response spectra was described and its feasibility was examined by several illustrative example calculations. From the

results of these preliminary studies, the following general remarks are presented:

- (1) By using the results of the statistical analysis of acceleration response spectra^(2,3) as an attenuation law, the seismic risk of a site may be evaluated in terms of elastic response of SDOF structures. The method incorporates the effects of the ground condition of the site and the magnitudes and distances of causative earthquakes on the frequency characteristics as well as the intensity of ground motion.
- (2) The seismic risk thus evaluated contains more information than the risk expressed in terms of a certain peak amplitude of ground motion. The method also allows one to assess the relative importance of different earthquake sources on the total seismic risk of structures with different natural periods.
- (3) According to the result of the preliminary analysis, the seismic risk of long-period structures seems to be more uniformly distributed over the whole area of Japan than that of short-period structures.

REFERENCES CITED

- (1) T. Katayama, "Engineering prediction of acceleration response spectra and its application to seismic risk analysis", Proc. 5th Japan Earthquake Eng. Sym.-1978, Nov., 1978.
- (2) T. Katayama, T. Iwasaki and M. Saeki, "Prediction of acceleration response spectra for given earthquake magnitude, epicentral distance and site conditions", Bull. Earthquake Resistant Structure Res. Center, Inst. of Ind. Sci., Univ. of Tokyo, No.11, Dec., 1977.
- (3) T. Katayama, T. Iwasaki and M. Saeki, "Statistical analysis of earthquake acceleration response spectra (in Japanese)", Proc. JSCE, No.275, July, 1978.

(Manuscript was received on Dec. 18, 1978)

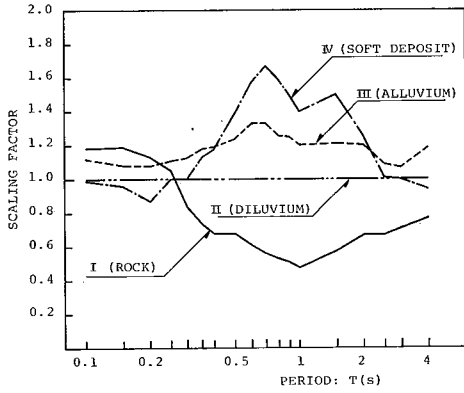


Fig.1. Scaling Factors for Different Ground Conditions

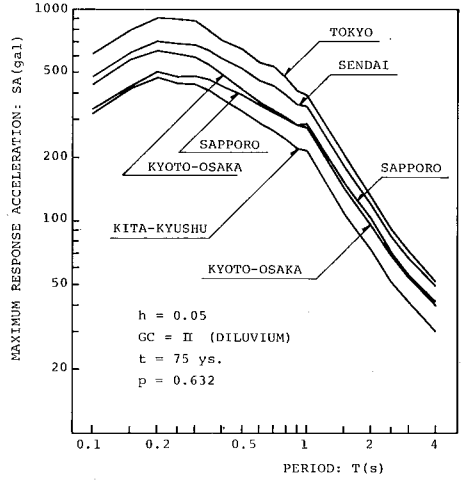


Fig.2. Expected Acceleration Response Spectra for the Five Sites

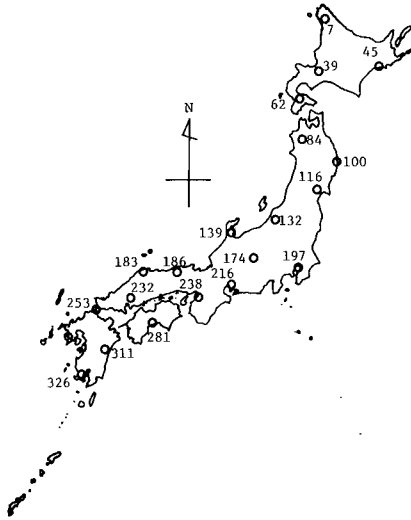


Fig.3. Twenty Selected Sites for Preliminary Study

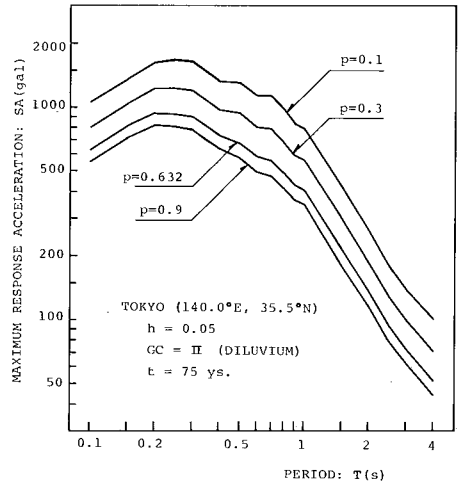


Fig.4. Examples of Computed Acceleration Response Spectra for Tokyo (I)

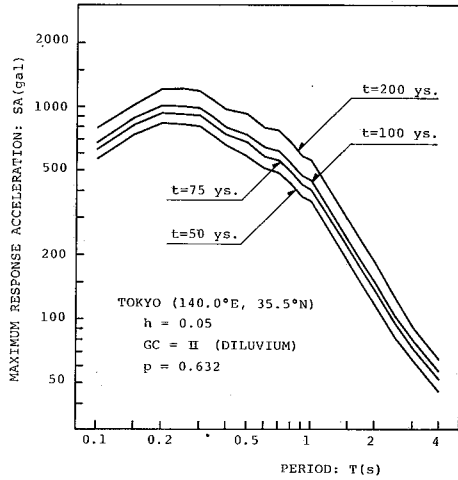


Fig.5. Examples of Computed Acceleration Response Spectra for Tokyo (II)

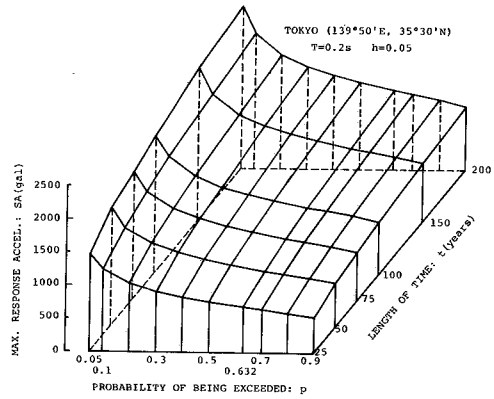


Fig.6. An Example of Variation of Spectral Amplitude with t and P

Table 1. Distance and Magnitude Classifications

Distance Range		Magnitude Range	
D1	$0 \leq \Delta < 20$	M1	$4.5 \leq M < 5.4$
D2	$20 \leq \Delta < 60$	M2	$5.4 \leq M < 6.1$
D3	$60 \leq \Delta < 120$	M3	$6.1 \leq M < 6.7$
D4	$120 \leq \Delta < 200$	M4	$6.7 \leq M < 7.5$
D5	$200 \leq \Delta < 350$	M5	$7.5 \leq M$

Table 2.

Relative Contributions (in Percent) from Different Earthquake Sources to Seismic Risk ($h=0.05$, $t=75$ and $p=0.632$).

T (s)	Sapporo			Sendai			Tokyo			Kyoto-Osaka			Kita-Kyushu		
	D1 D2	D3 D3	D4 D5	D1 D2	D3 D3	D4 D5	D1 D2	D3 D3	D4 D5	D1 D2	D3 D3	D4 D5	D1 D2	D3 D3	D4 D5
0.2	40	23	37	50	38	12	80	17	3	60	33	7	58	27	15
0.5	34	13	53	53	18	29	83	9	8	46	24	30	54	15	31
1.0	22	12	66	34	22	44	68	15	17	28	28	44	40	16	44
2.0	19	11	70	27	23	50	60	16	24	24	30	46	37	15	48
4.0	14	11	75	17	26	57	40	20	40	17	33	50	27	17	56

Table 3. Summary of Seismic Risk of 20 Sites Investigated

(1)	(2)	(3)		(4)	(5)	(6)	(7)	(8)	(9)
Site No.	Site Name	Lat. (°N)	Long. (°E)	T=0.2s		T=1.0s		T=4.0s	
				Accel (gal)	Ratio to Tokyo	Accel (gal)	Ratio to Tokyo	Accel (gal)	Ratio to Tokyo
7	Wakkanai	45.0	142.0	431	0.46	236	0.58	33.6	0.65
39	Sapporo	43.0	141.5	526	0.56	288	0.71	42.4	0.82
45	Kushiro	43.0	144.5	797	0.86	385	0.95	49.7	0.97
62	Hakodate	42.0	140.5	531	0.57	286	0.70	41.1	0.80
84	Hirosaki	40.5	140.5	573	0.62	311	0.76	45.6	0.89
100	Miyako	39.5	142.0	833	0.89	386	0.95	52.1	1.01
116	Sendai	38.5	141.0	771	0.83	368	0.90	51.0	0.99
132	Niigata	37.5	139.0	606	0.65	301	0.74	44.4	0.86
139	Nanao	37.0	137.0	571	0.61	263	0.65	38.3	0.74
174	Suwa	36.0	138.0	710	0.76	300	0.73	43.5	0.84
183	Matsue	35.5	133.0	547	0.59	240	0.59	33.6	0.65
186	Tottori	35.5	134.5	604	0.65	276	0.68	38.7	0.75
197	Tokyo	35.5	140.0	<u>931</u>	<u>1.00</u>	<u>407</u>	<u>1.00</u>	<u>51.5</u>	<u>1.00</u>
216	Nagoya	35.0	137.0	684	0.73	320	0.79	44.5	0.86
232	Hiroshima	34.5	132.5	552	0.59	252	0.62	36.2	0.70
238	Izumi	34.5	135.5	618	0.66	270	0.66	38.5	0.75
253	Shimonoseki	34.0	131.0	474	0.51	218	0.54	30.7	0.60
281	Kochi	33.5	133.5	528	0.57	248	0.61	37.0	0.72
311	Hyuga	32.5	131.5	673	0.72	269	0.66	35.2	0.68
326	Kagoshima	31.5	130.5	544	0.58	233	0.57	32.2	0.63